LITERATURE CITED

Davidson, J. F., and D. Harrison, *Fluidized Particles,* Cambridge Univ. Press, Cambridge, England (1963).

Fryer, C., "Fluidized Bed Reactors—Behaviour and Design," Ph.D. thesis, Monash University, Australia (1974).

———., and O. E. Potter, "Countercurrent Backmixing Model for Fluidized Bed Catalytic Reactors. Applicability of Simplified Solutions," *Ind. Eng. Chem. Fundamentals,* **11**, 338 (1972*a*).

————, "Bubble Size Variation in Two-Phase Models of Fluidized Bed Reactors," *Powder Technol.,* **6**, 317 (1972*b*).

————, "Fluidized Bed Reactor Performance—An Experimental Study of the Countercurrent Backmixing Model," *Proc. Internat. Symp. on Fluidization and its Applications,* Toulouse (Oct., 1973). Ste. Chimie Industrielle, page 440 (1974).

Harrison, D., and L. S. Leung, "Bubble Formation at an Orifice in a Fluidised Bed," *Trans. Inst. Chem. Engrs.,* **39**, 409 (1961).

Kato, K., and C. Y. Wen, "Bubble Assemblage Model for Fluidized Bed Catalytic Reactors," *Chem. Eng. Sci.,* **24**, 1351 (1969).

Kobayashi, H., F. Arai, and T. Chiba, "Behaviour of Bubbles in a Gas-Solid Fluidized Bed," *Kagaku Kogaku (Eng. Edition),* **4**, 147 (1966).

Kunii, D., and O. Levenspiel, "Bubbling Bed Model. Model for Flow of Gas through a Fluidized Bed," *Ind. Eng. Chem. Fundamentals,* **7**, 446 (1968).

Latham, R. L., C. J. Hamilton, and O. E. Potter, "Backmixing and Chemical Reaction in Fluidised Beds," *Brit. Chem. Eng.,* **13**, 666 (1968).

Perry, J. H., *Chemical Engineers' Handbook,* 3 ed., McGraw-Hill, New York (1950).

Potter, O. E., "Mixing," in *Fluidization,* Chapt. 7, J. F. Davidson and D. Harrison, ed., Academic Press, London (1971).

Schügerl, K., Discussion in *Proc. Internat. Symp. on Fluidization and its Applications,* Toulouse, (Oct., 1973). Ste. Chimie Industrielle, page 712 (1974).

Stephens, G. K., R. J. Sinclair, and O. E. Potter, *Powder Technol.,* **1**, 61 (1967).

Whitehead, A. B., and A. D. Young, "Fluidization Performance in Large-Scale Equipment," *Proc. Internat. Symp. on Fluidization,* Eindhoven (June, 1967). A. A. Drinkenburg, ed., page 284, Netherlands University Press, Amsterdam (1967).

A Model for Predicting Flow Regime Transitions in Horizontal and Near Horizontal Gas-Liquid Flow

Models are presented for determining flow regime transitions in two-phase gas-liquid flow. The mechanisms for transition are based on physical concepts and are fully predictive in that no flow regime transitions are used in their development. A generalized flow regime map based on this theory is presented.

YEMADA TAITEL
and
A. E. DUKLER

Department of Chemical Engineering
University of Houston
Houston, Texas 77004

SCOPE

Predicting the flow regime for concurrent gas liquid flow in pipes has been a central unresolved problem in two-phase flow. The usual approach has been to collect data for flow rates and fluid properties and to visually observe the flow pattern through a transparent test section window. Then a search is undertaken for a way to map the data in a two-dimensional plot by locating transition boundaries between the regimes. This requires a decision to be made about the coordinates which are used. Because no theoretical basis for selection of coordinates has existed in the past, this approach represents a coordination of the data rather then a correlation and depends strongly on the particular data being used to prepare the map. For this reason extension to other conditions of pipe size or inclination, fluid properties, and flow rates are of uncertain reliability.

This work has the objective of presenting a means for unambiguous analytical prediction of the transition between flow regimes based on physically realistic mechanisms for these transitions. The regimes considered are intermittent (slug and plug), stratified smooth, stratified wavy, dispersed bubble, and annular-annular dispersed liquid flow. The theory predicts the effect on transition boundaries of pipe size, fluid properties, and angle of inclination.

CONCLUSIONS AND SIGNIFICANCE

A theoretical model is developed which predicts the relationship between the following variables at which flow regime transitions take place: gas and liquid mass flow rates, properties of the fluids, pipe diameter, and angle of inclination to the horizontal. The mechanisms for transition are based on physical concepts and are fully predictive in that no flow regime data are used in their development.

Five basic flow regimes are considered. When the theory is solved in dimensionless form the following

dimensionless groups emerge:

$$X = \left[\frac{|(dP/dx)_L{}^S|}{|(dP/dx)_G{}^S|} \right]^{1/2}$$

$$T = \left[\frac{|(dP/dx)_L{}^S|}{(\rho_L - \rho_G) g \cos \alpha} \right]^{1/2}$$

$$Y = \frac{(\rho_L - \rho_G) g \sin \alpha}{|(dP/dx)_G{}^S|}$$

$$F = \sqrt{\frac{\rho_G}{\rho_L - \rho_G}} \frac{U_G{}^S}{\sqrt{Dg \cos \alpha}}$$

$$K = F \left[\frac{DU_L{}^S}{\nu_L} \right]^{1/2} = F\,[Re_L{}^s]^{1/2}$$

All of these quantities can be determined from operating conditions, since velocities and pressure gradients are calculated from superficial conditions.

The particular transitions are shown to be controlled by the following groups:

Stratified to annular	X, F, Y
Stratified to intermittent	X, F, Y
Intermittent to dispersed bubble	X, T, Y
Stratified smooth to stratified wavy	X, K, Y
Annular dispersed liquid to intermittent and to dispersed bubble	X, Y

The theoretically located transition boundaries for $Y = 0$ (horizontal tube) are shown as a generalized two-dimensional map in Figure 4. Similar maps can be developed simply for any other value of Y by using hand calculations from the equations and graphical results given in the paper. Figure 5 shows that the agreement between these theoretical predictions and the latest available maps in which the predictions are located from the data is very good.

A parametric study was executed for the effect of operating variables on the regime boundaries in a two-dimensional map having as coordinates the superficial velocity of the gas and liquid. With this method of mapping, the boundaries are relatively insensitive to pipe diameter for an air-water system at low pressure and small line sizes. However, large shifts in location of some of the boundaries take place for larger line sizes, for gases at high pressure, and for slight inclinations from the horizontal. The new generalized map, such as Figure 4, does account for all of these operational factors and thus should permit the prediction of flow regime with confidence at conditions other than those determined in laboratory experiments.

The earliest and perhaps the most durable of regime maps for two-phase gas-liquid flow was proposed by Baker (1954). Many have been suggested (White and Huntington, 1955; Govier and Omer, 1962; Kosterin, 1949). Al-Sheikh et al. (1970) defined a variety of dimensionless groups and using the Dukler two-phase flow data bank evaluated the suitability of various pairs for mapping the flow regimes. They concluded that no two groups characterized all of the transitions and all of the data. Recently a mapping based on coordinates of superficial gas and liquid velocity has been constructed from a larger data base (Mandhane et al., 1974).

Part of the problem arises from the lack of precision in describing these visual observations. There have been innumerable classifications suggested, such as smooth stratified, wavy, semiannular, bubble, annular, froth, dispersed bubble, dispersed liquid, plug, and slug flow, among others. Hubbard and Dukler (1966), based on studies of the spectral distribution of wall pressure fluctuations, suggested that each observation represents the superposition of three basic patterns: separated, intermittent, and distributed flow. However, the concept does not discriminate between stratified and annular flow, or between the dispersed liquid or dispersed gas flow regimes, and these are differences of considerable practical concern.

In this work a mechanistic model is developed for the unambiguous analytical prediction of transition between flow regimes. This approach also provides considerable insight into the mechanisms of the transitions.

THEORY

The analysis which follows considers the conditions for transition between five basic flow regimes: (*SS*) smooth stratified, (*SW*) wavy stratified, (*I*) intermittent (slug and plug), (*AD*) annular with dispersed liquid, and (*DB*) dispersed bubble. No distinction is made between slug, plug, or elongated bubble flows, all being considered different conditions of the intermittent flow regime (Dukler and Hubbard, 1975). Annular dispersed liquid flow represents the condition described in the past of annular or semiannular with various degrees of liquid entrainment ranging between very small and large amounts of dispersed liquid.

The process of analyzing the transitions between flow regimes starts from the condition of stratified flow. The approach is to visualize a stratified liquid and then to determine the mechanism by which a change from stratified flow can be expected to take place, as well as the flow pattern that can be expected to result from the change. In many cases stratified flow is seen to actually exist in the entry region of the pipe. However, the fact that stratified flow may not actually exist is not important, since it is well established that the existence of a specific flow pattern at specified gas and liquid rates is independent of the path used to arrive at that state.

Since the condition of stratified flow is central to this analysis, the initial step is the development of a generalized relationship for stratified flows.

Equilibrium Stratified Flow

Consider smooth, equilibrium stratified flow as shown in Figure 1. A momentum balance on each phase yields

$$-A_L \left(\frac{dP}{dx} \right) - \tau_{WL} S_L + \tau_i S_i + \rho_L A_L g \sin \alpha = 0 \quad (1)$$

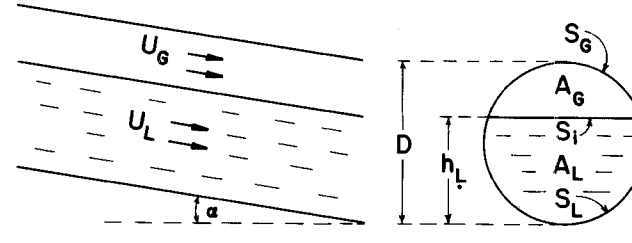

Fig. 1. Equilibrium stratified flow.

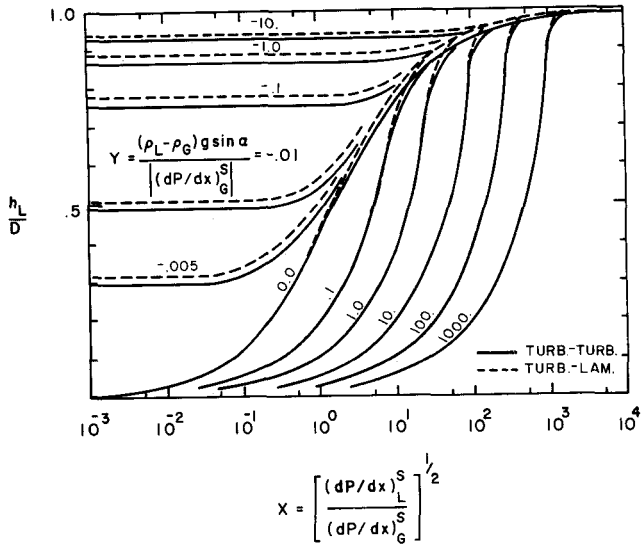

Fig. 2. Equilibrium liquid level for stratified flow (turbulent liquid, turbulent or laminar gas).

$$-A_G\left(\frac{dP}{dx}\right) - \tau_{WG}S_G - \tau_i S_i + \rho_G A_G \sin\alpha = 0 \quad (2)$$

Equating pressure drop in the two phases and assuming that at transition conditions the hydraulic gradient in the liquid is negligible, gives the following results

$$\tau_{WG}\frac{S_G}{A_G} - \tau_{WL}\frac{S_L}{A_L} + \tau_i S_i\left(\frac{1}{A_L}+\frac{1}{A_G}\right) + (\rho_L - \rho_G)\, g \sin\alpha = 0 \quad (3)$$

The shear stresses are evaluated in a conventional manner

$$\tau_{WL} = f_L\frac{\rho_L u_L^2}{2} \quad \tau_{WG} = f_G\frac{\rho_G u_G^2}{2} \quad \tau_i = f_i\frac{\rho_G(u_G-u_i)^2}{2} \quad (4)$$

with the liquid and gas friction factors evaluated from

$$f_L = C_L\left(\frac{D_L u_L}{\nu_L}\right)^{-n} \quad f_G = C_G\left(\frac{D_G u_G}{\nu_G}\right)^{-m} \quad (5)$$

where D_L and D_G are the hydraulic diameter evaluated in the manner as suggested by Agrawal et al. (1973):

$$D_L = \frac{4A_L}{S_L} \quad D_G = \frac{4A_G}{S_G + S_i} \quad (6)$$

This implies that the wall resistance of the liquid is similar to that for open-channel flow and that of the gas to closed-duct flow. It has been established that for smooth stratified flow, $f_i \simeq f_G$ (Gazley, 1949). Even though many of the transitions considered here take place in stratified flow with a wavy interface, the error incurred by making this assumption is small. At flow rate conditions, where transitions are observed to take place, $u_G >> u_i$. Thus, the gas side interfacial shear stress is evaluated with the same equation as the gas wall shear. In this work the following coefficients were utilized: $C_G = C_L = 0.046$, $n = m = 0.2$ for the turbulent flow and $C_G = C_L = 16$, $n = m = 1.0$ for laminar flow.

It is useful to transform these equations to dimensionless form. The reference variables are: D for length, D^2 for area, the superficial velocities, $u_L{}^S$ and $u_G{}^S$ for the liquid and gas velocities, respectively. By designating the dimensionless quantities by a tilde ($\sim$), Equation (3) with (4) and (5) takes the form

$$X^2\left[(\tilde{u}_L\tilde{D}_L)^{-n}\tilde{u}_L{}^2\frac{\tilde{S}_L}{\tilde{A}_L}\right] - \left[(\tilde{u}_G\tilde{D}_G)^{-m}\tilde{u}_G{}^2\left(\frac{\tilde{S}_G}{\tilde{A}_G}+\frac{\tilde{S}_i}{\tilde{A}_L}+\frac{\tilde{S}_i}{\tilde{A}_G}\right)\right] - 4Y = 0 \quad (7)$$

where

$$X^2 = \frac{\frac{4C_L}{D}\left(\frac{u_L{}^S D}{\nu_L}\right)^{-n}\frac{\rho_L(u_L{}^S)^2}{2}}{\frac{4C_G}{D}\left(\frac{u_G{}^S D}{\nu_G}\right)^{-m}\frac{\rho_G(u_G{}^S)^2}{2}} = \frac{|(dP/dx)_L{}^S|}{|(dP/dx)_G{}^S|} \quad (8)$$

$$Y = \frac{(\rho_L-\rho_G)g\sin\alpha}{\frac{4C_G}{D}\left(\frac{u_G{}^S D}{\nu_G}\right)^{-m}\frac{\rho_G(u_G{}^S)^2}{2}} = \frac{(\rho_L-\rho_G)g\sin\alpha}{|(dP/dx)_G{}^S|} \quad (9)$$

$|(dP/dx)^s|$ designates the pressure drop of one phase flowing alone in the pipe. Thus, X is recognized as the parameter introduced by Lockhart and Martinelli (1949) and can be calculated unambiguously with the knowledge of flow rates, fluid properties, and tube diameter. Y is zero for horizontal tubes and represents the relative forces acting on the liquid in the flow direction due to gravity and pressure drop. It too can be calculated directly. All dimensionless variables with the superscript $\sim$ depend only on $\tilde{h}_L = h_L/D$, as can be seen from

$$\tilde{A}_L = 0.25\,[\pi - \cos^{-1}(2\tilde{h}_L - 1) + (2\tilde{h}_L - 1)\sqrt{1-(2\tilde{h}_L-1)^2}] \quad (10)$$

$$\tilde{A}_G = 0.25\,[\cos^{-1}(2\tilde{h}_L - 1) - (2\tilde{h}_L - 1)\sqrt{1-(2\tilde{h}_L-1)^2}] \quad (11)$$

$$\tilde{S}_L = \pi - \cos^{-1}(2\tilde{h}_L - 1) \quad (12)$$

$$\tilde{S}_G = \cos^{-1}(2\tilde{h}_L - 1) \quad (13)$$

$$\tilde{S}_i = \sqrt{1-(2\tilde{h}_L-1)^2} \quad (14)$$

$$\tilde{u}_L = \tilde{A}/\tilde{A}_L \quad (15)$$

$$\tilde{u}_G = \tilde{A}/\tilde{A}_G \quad (16)$$

Thus, each X-Y pair corresponds to a unique value of h_L/D for all conditions of pipe size, fluid properties, flow rate, and pipe inclinations for which stratified flow exists. The solution of Equation (7) has been executed for turbulent flow of both phases, which is clearly the case of greatest practical interest ($n = m = 0.2$, $C_G = C_L = 0.046$). The results are shown as the solid curves in Figure 2. Other situations may be readily solved from Equation (7) by utilizing the applicable coefficients. The case for turbulent liquid with laminar gas flow can occur in practice for transitions which take place at low gas rates. The solutions for $n = 0.2$, $m = 1$, $C_L = 0.046$, $C_G = 16$ is shown dotted in Figure 2 and is remarkably close to the turbulent/turbulent case. It should be noted that the decision on whether laminar or turbulent flow takes place in each phase should be based on the Reynolds number calculated by using the

actual velocity and hydraulic diameter of this phase, not the superficial velocity and diameter.

Transition Between Stratified (S) and Intermittent (I) or Annular-Dispersed Liquid (AD) Regimes

Extensive experimental and analytical studies (Dukler and Hubbard, 1975) have shown that for the range of flow conditions over which intermittent flow is observed, the flow at the inlet of the pipe is, at first, stratified. As the liquid rate is increased, the liquid level rises and a wave is formed which grows rapidly tending to block the flow. At lower gas rates, the blockage forms a competent bridge, and slug or plug flow ensues. At higher gas rates, there is insufficient liquid flowing to maintain or, in some cases, even to form the liquid bridge, and the liquid in the wave is swept up and around the pipe to form an annulus with some entrainment if the gas rate is high enough. Butterworth (1972) has demonstrated this mechanism for annular film formation. Thus, this transition can be defined as that from stratified flow to either intermittent or annular flow. It takes place when the conditions are such that a finite amplitude wave on the stratified surface will grow. This transition can be expected to be sharply defined as observed in practice.

Consider stratified flow with a wave existing on the surface over which gas flows. As the gas accelerates, the pressure in the gas phase over the wave decreases owing to the Bernoulli effect, and this tends to cause the wave to grow. The force of the gravity acting on the wave tends to make it decay. The Kelvin-Helmholtz theory (Milne-Thomson, 1960) provides a stability criteria for waves of infinitesimal amplitude formed on a flat sheet of liquid flowing between horizontal parallel plates. According to this theory, waves will grow when

$$u_G > \left[\frac{g(\rho_L - \rho_G)h_G}{\rho_G}\right]^{1/2} \tag{17}$$

where h_G is the distance between the upper plate and the equilibrium liquid level.

This type of stability analysis is now extended in a rather elementary manner, first to the case of a finite wave on a flat liquid sheet between parallel plates and then to finite waves on stratified liquid in an inclined pipe. Consider a finite solitary wave on a flat horizontal surface, as shown in Figure 3, having a peak height h_L' and a gas gap dimension h_G'. The equilibrium dimensions are h_L and h_G. If the motion of the wave is neglected, the condition for wave growth is

$$P - P' > (h_G - h_G')(\rho_L - \rho_G)g \tag{18}$$

with

$$P - P' = \tfrac{1}{2}\rho_G(u_G'^2 - u_G^2) \tag{19}$$

The criterion for instability then becomes

$$u_G > C_1\left(\frac{g(\rho_L - \rho_G)h_G}{\rho_G}\right)^{1/2} \tag{20}$$

where C_1 depends on the size of the wave:

$$C_1 = \left[\frac{2}{\frac{h_G}{h_G'}\left(\frac{h_G}{h_G'} + 1\right)}\right]^{1/2} \tag{21}$$

For infinitesimal disturbance, $h_G/h_G' \to 1.0$, $C_1 \to 1.0$, and Equation (20) reduces to (17). However, a comparison of these two equations shows that finite disturbances are less stable than infinitesimal ones, since for a finite disturbance C_1 is less than unity.

Wallis and Dobson (1973) arrived at Equation (20) with $C = 0.5$ from observation of experimental data. Using qualitative arguments, they extended Benjamin's (1968) work for flow of liquid around a gas cavity to the idea of a flow gas over a wave to attempt to justify this value of the coefficient. However, their arguments are questionable for this application because the inversion of gas and liquid has little theoretical basis in this procedure.

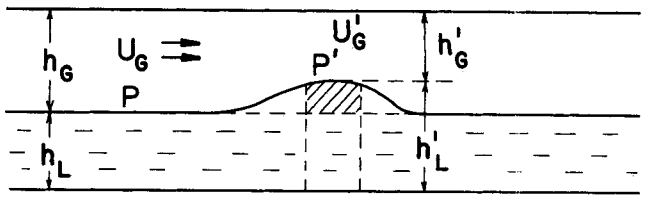

Fig. 3. Instability for a solitary wave.

This simple analysis can be easily extended to the round pipe geometry and to inclined pipes to give

$$u_G > \left[\frac{2(\rho_L - \rho_G)g\cos\alpha\,(h_L' - h_L)}{\rho_G}\,\frac{A_G'^2}{A_G^2 - A_G'^2}\right]^{1/2} \tag{22}$$

For small, though finite, disturbances, A_G' can be expanded in a Taylor series around A_G to yield

$$u_G > C_2\left[\frac{(\rho_L - \rho_G)g\cos\alpha\,A_G}{\rho_G\;dA_L/dh_L}\right]^{1/2} \tag{23}$$

where $C_2 \simeq A_G'/A_G$. C_2 is seen to be unity for the infinitesimal disturbance where $A_G' \to A_G$. When the equilibrium liquid level approaches the top of the pipe and A_G is small, any wave of finite amplitude which appears will cause $C_2 \simeq A_G'/A_G$ to approach zero. Conversely, for low levels the appearance of a small finite amplitude wave will have little effect on the air gap size, and C_2 approaches 1.0. For this reason we speculate that C_2 can be estimated as follows:

$$C_2 = 1 - \frac{h_L}{D} \tag{24}$$

Note that for $h_L/D = 0.5$, C_2 equals 0.5, and this is consistent with the result of Wallis and Dobson (1973). Kordyban and Ranov (1970) analyzed the transition from stratified to slug flow for water and air between horizontal parallel plates. Their data for air velocity to effect transition as a function of the channel air and water gaps gives close agreement with Equation (20), using C_1 given by Equation (24). Thus it is suggested that Equations (23) and (24) describe the conditions for the transition in pipes from stratified (S) to intermittent (I) and to annular dispersed liquid (AD) flow.

In dimensionless form the criterion becomes

$$F^2\left[\frac{1}{C_2^2}\,\frac{\tilde{u}_G\,d\tilde{A}_L/d\tilde{h}_L}{\tilde{A}_G}\right] \geq 1 \tag{25}$$

where F is a Froude number modified by the density ratio:

$$F = \sqrt{\frac{\rho_G}{(\rho_L - \rho_G)}}\,\frac{u_G^s}{\sqrt{Dg\cos\alpha}} \tag{26}$$

Note that all terms in the square brackets of Equation (25) are functions of h_L/D which is, in turn, a unique function of the dimensionless groups X and Y as shown in Figure 2. Thus this transition is uniquely determined by three dimensionless groups X, Y, and F. For any specified value of Y, the transition is uniquely determined by X and F and can be represented on a generalized two-dimensional map. For example, for horizontal flow a series of values

of X were selected, and the corresponding values of h_L/D were determined from Figure 2. The bracketed term in Equation (25) can then be calculated for each h_L/D by using Equations (11), (16), and (24) and the following expression:

$$\frac{d\tilde{A}_L}{d\tilde{h}_L} = \sqrt{1 - (2\tilde{h}_L - 1)^2} \tag{27}$$

Then the value of F required to satisfy the equality in Equation (25) can be calculated. The curve describing the relation between X and F which satisfies Equation (25) for horizontal flow is designated as boundary A in Figure 4. The region to the left of this curve represents stratified flow. Although not presented here, it is a simple matter to repeat the calculation described above for inclined pipes by specifying other values of Y and by using the corresponding curve in Figure 2.

Transition Between Intermittent (I) and Annular Dispersed Liquid (AD) Regimes

Equation (25) presents the criteria under which finite waves which appear on the stratified liquid can be expected to grow. Two events can take place when such a growth is observed. A stable slug can form when the supply of liquid in the film is large enough to provide the liquid needed to maintain such a slug. When the level is inadequate, the wave is swept up around the wall as described by Butterworth (1972), and annular or annular mist flow takes place. This suggests that whether intermittent or annular flow will develop depends uniquely on the liquid level in the stratified equilibrium flow. It is suggested that when the equilibrium liquid level in the pipe is above the pipe center line, intermittent flow will develop, and if $h_L/D < 0.5$, annular or annular dispersed liquid flow will result. This choice of $h_L/D = 0.5$ can be explained as follows. When a finite amplitude wave begins to grow as a result of the suction over the crest of the wave, liquid must be supplied from the fluid in the film adjacent to the wave, and a depression or trough forms there. Picture the wave as a sinusoid. If the level is above the center line, the peak of the wave will reach the top before the trough reaches the bottom of the pipe, and then blockage of the gas passage and slugging results. When the liquid level is below the center line, the inverse will be true, which will make slugging impossible.

Since transition takes place at a constant value of $h_L/D = 0.5$, a single value of X characterizes the change in regime for any value of Y (Figure 2). For horizontal tubes, this value is $X = 1.6$, and this is plotted in Figure 4 as boundary B. Note that the location of this curve now defines two possible transitions as one moves across boundary A: from stratified to intermittent (S/I) for values of X greater than $X = 1.6$ and stratified to annular dispersed liquid (S/AD) for values of X less than $X = 1.6$.

Unlike the transition between stratified and intermittent flow for which the mechanism suggests a sharp, well-defined change, this transition is a gradual one since it is not possible to distinguish between a highly aerated slug and annular flow with large roll waves.

Transition Between Stratified Smooth (SS) and Stratified Wavy (SW) Regimes

The region designated above as a stratified regime includes two subregions: stratified smooth (SS) and stratified wavy (SW). These waves are caused by the gas flow under conditions where the velocity of the gas is sufficient to cause waves to form but slower than that needed for the rapid wave growth which causes transition to intermittent or annular flow.

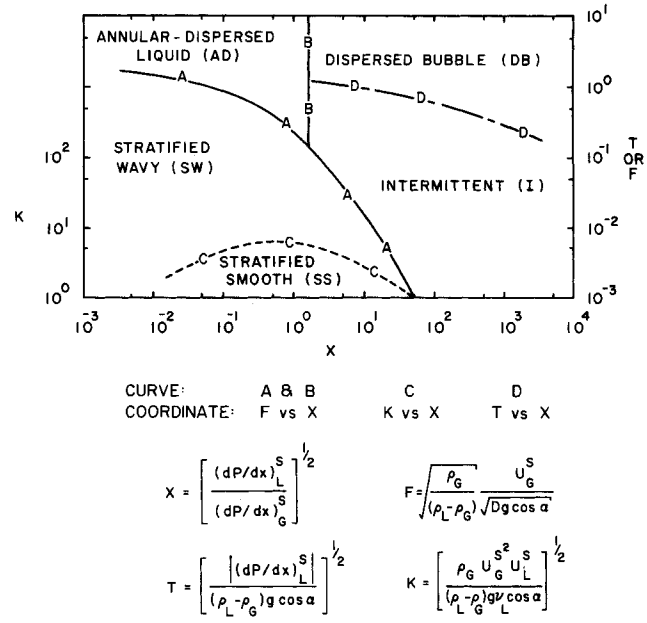

Fig. 4. Generalized flow regime map for horizontal two-phase flow.

The phenomenon of wave generation is quite complicated and not completely understood. It is generally accepted that waves will be initiated when pressure and shear work on a wave can overcome the viscous dissipation in the waves. However, there is considerable controversy over the mechanism by which the energy transfer takes place. A good summary is provided by Stewart (1967).

In this work we use the ideas introduced by Jeffreys (1925, 1926) who suggested the following condition for wave generation:

$$(u_G - c)^2\, c > \frac{4\nu_L g(\rho_L - \rho_G)}{s\,\rho_G} \tag{28}$$

In this equation s is a sheltering coefficient which Jeffreys suggested should take a value of about 0.3. However, based on theory as well as on experimental results for flow and fixed wavy surfaces, Benjamin (1959) indicated much smaller values for this coefficient ranging from 0.01 to 0.03. For this work the value of $s = 0.01$ is used.

c is the velocity of propagation of the waves. For most conditions where transition can be expected to take place, $u_G >> c$. Theories concerning these waves suggest that the ratio of the wave velocity to the mean of the film velocity c/u_L decreases with increasing Reynolds number of the liquid, and the data of Fulford (1964), Brock (1970) and Chu (1973) confirm this. At the high Reynolds numbers associated with turbulent liquid flow taking place near these transitions, the ratio approaches 1.0 to 1.5. For simplicity, and because a precise location of this transition boundary is not important, the relation $u_L = c$ is used.

These approximations substituted into Equation (28) give the criterion for this transition:

$$u_G \geq \left[\frac{4\,\nu_L(\rho_L - \rho_G)g\cos\alpha}{s\,\rho_G u_L}\right]^{1/2} \tag{29}$$

In dimensionless form this can be expressed as

$$K \geq \frac{2}{\sqrt{\tilde{u}_L}\,\tilde{u}_G\sqrt{s}} \tag{30}$$

where K is the product of the modified Froude number and the square root of the superficial Reynolds number of the liquid:

$$K^2 = F^2 Re_L{}^s = \left[\frac{\rho_G (u_G{}^s)^2}{(\rho_L - \rho_G) D g \cos \alpha} \right] \left[\frac{D u_L{}^s}{\nu_L} \right] \tag{31}$$

Since $\tilde{u}_L$ and $\tilde{u}_G$ depend only on h_L/D [see Equations (15) and (16)], they are determined once X and Y are specified. Thus this transition between smooth and wavy annular flow depends on the three parameters K, X, and Y. For any fixed inclination, this becomes a two-parameter dependence on X and K. The relationship which satisfies the equality of Equation (30) can conveniently be mapped in Figure 4 by designating a differently scaled ordinate than that which applies to the two transitions discussed previously. Curve C shows the results for $Y = 0$ ($s = 0.01$).

While the location of this transition curve is approximate, it is important to note that it is based on a physically realistic model. Should it be necessary to locate the curve more accurately, this would be possible once additional data on c/u_L and s are available. However, the result depends on each of these quantities to the one-half power and thus is relatively insensitive to changes.

Transition Between Intermittent (I) and Dispersed Bubble (DB) Regimes

For values of X in Figure 4 to the right of boundaries A and B, waves will tend to bridge the pipe forming a liquid slug and an adjacent gas bubble. At high liquid rates and low gas rates, the equilibrium liquid level approaches the top of the pipe, as is apparent from Figure 2. With such a fast running liquid stream the gas tends to mix with the liquid, and it is suggested that the transition to dispersed bubble flow takes place when the turbulent fluctuations are strong enough to overcome the buoyant forces tending to keep the gas at the top of the pipe.

The force of buoyancy per unit length of the gas region is

$$F_B = g \cos \alpha \, (\rho_L - \rho_G) A_G \tag{32}$$

In a manner used by Levich (1962), the force acting because of turbulence is estimated to be

$$F_T = \tfrac{1}{2} \rho_L \overline{v'^2} \, S_i \tag{33}$$

where v' is the radial velocity fluctuation whose root-mean-square is estimated to be approximately equal to the friction velocity. Thus

$$\overline{v'^2}^{1/2} = u_* = u_L \left(\frac{f_L}{2} \right)^{1/2} \tag{34}$$

Dispersion of the gas is visualized as taking place when $F_T \geq F_B$, or

$$u_L \geq \left[\frac{4 A_G}{S_i} \frac{g \cos \alpha}{f_L} \left(1 - \frac{\rho_G}{\rho_L} \right) \right]^{1/2} \tag{35}$$

In a dimensionless form, Equation (35) takes the form

$$T^2 \geq \left[\frac{8 \tilde{A}_G}{\tilde{S}_i \, \tilde{u}_L{}^2 \, (\tilde{u}_L \tilde{D}_L)^{-n}} \right] \tag{36}$$

where

$$T = \left[\frac{\frac{4 C_L}{D} \left(\frac{u_L{}^s D}{\nu_L} \right)^{-n} \frac{\rho_L u_L{}^{s2}}{2}}{(\rho_L - \rho_G) g \cos \alpha} \right]^{1/2} = \left[\frac{|(dP/dx)_L{}^s|}{(\rho_L - \rho_G) g \cos \alpha} \right]^{1/2} \tag{37}$$

T can be considered as the ratio of turbulent to gravity forces acting on the gas.

The terms in the square bracket in Equation (36) are again dependent only on h_L/D and thus on X and Y. For any specific value of Y, a two-dimensional representation for this transition is possible, with X and T used as the dimensionless coordinates. It is possible to map this transition on Figure 4 by using the common X abscissa and T as an ordinate as shown by curve D calculated for $Y = 0$.

RESULTS

The Generalized Flow Regime Map

The generalized flow regime map for the case of horizontal tubes ($Y = 0$) appears in Figure 4. Curve A represents the transition from stratified (S) to intermittent (I) or annular-dispersed liquid (AD) flows, with the coordinates for curve A being F vs. X. The curve gives the locus of the F-X pairs which satisfies Equation (25) and results from the argument that waves of finite size will grow and tend to block or sweep around the pipe when the force due to the Bernoulli effect above the wave is greater than gravity force acting on the wave. Thus, all values of X to the left of the curve represent conditions under which stratified flow will exist.

Curve B locates the transition between intermittent (I) or dispersed bubble (DB) and annular-dispersed liquid (AD) flow. This occurs at a constant value of X resulting from the argument that the growing waves will have sufficient liquid supply to form a slug only when $h_L/D \geq 0.5$, and below that value they will be swept around the pipe into an annular configuration.

Curve C represents the transition between stratified smooth (SS) and stratified wavy (SW) flow. It is plotted in the K-X plane and locates the K-X pairs which satisfy Equation (30). The model is based on the assumption that the Jeffreys model is valid for describing the condition for transfer of energy to the liquid in order to create waves, with the wave velocity estimated from the mean velocity of the liquid film and the sheltering coefficient determined from an analysis of Benjamin. Any value of K lower than curve C in the K-X plane will provide insufficient gas flow to cause waves to form.

Curve D indicates the transition between intermittent and dispersed bubble flow. It represents an identification of conditions where the turbulent fluctuations in the liquid become equal to the buoyant forces which tend to make the gas rise to the top of the pipe. This curve gives the locus of the T-X pairs which satisfies Equations (36). All values of T below the curve represent conditions where turbulence is insufficient to keep the gas mixed, and the elongated gas bubbles characteristic of intermittent flow will form. The set of transition curves for other values of Y can easily be calculated from Figure 2 and the defining transition equations.

The effect of pipe roughness on these transitions is not specifically considered in the development. However, subject to experimental demonstration, it is suggested that if the $(dP/dx)^s$ values are calculated by using known roughness parameters, the transition boundaries of Figure 4 will continue to apply.

It is, of course, not necessary to use a flow regime map at all. Given any one set of flow conditions (rate, pressure, line size, and inclination), the flow pattern that exists for that condition can be determined rather simply by using hand calculations from Equation (25), (30), and (36) with the help of Figure 2.

Comparison with Data

Mandhane, Gregory and Aziz (1974) have recently made a careful examination of flow regime data. They showed that over 1 000 data points for the air-water system in horizontal pipes ranging in size from 1.3 to 15 cm

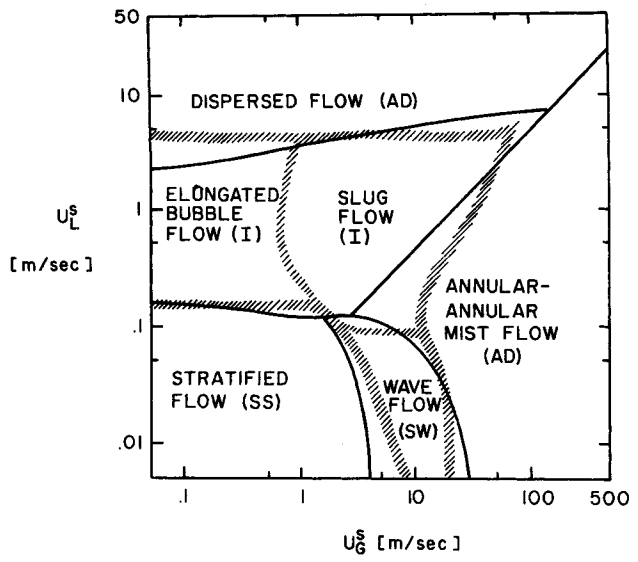

Fig. 5. Comparison of theory and experiment. Water-air, 25°C, 1 atm, 2.5 cm. diam., horizontal. ——— theory; //////// Mandhane et al. (1974). Regime descriptions as in Mandhane.

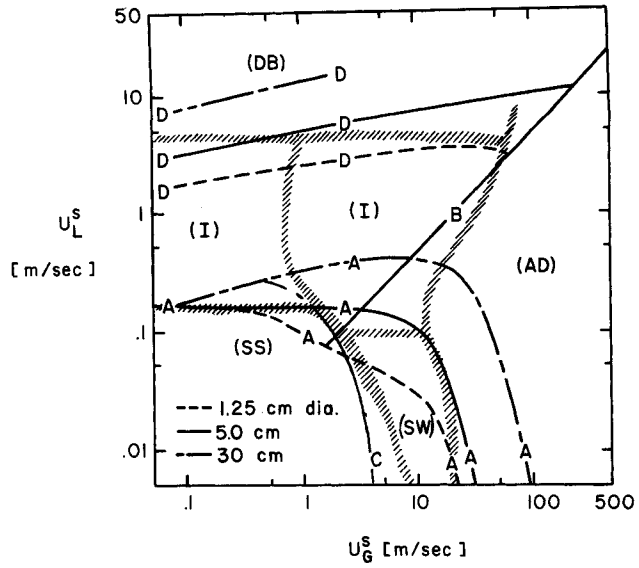

Fig. 6. Effect of pipe diameter on transition boundaries. Water-air, 25°C, 1 atm, horizontal. ——— theory; //////Mandhane et al. (1974).

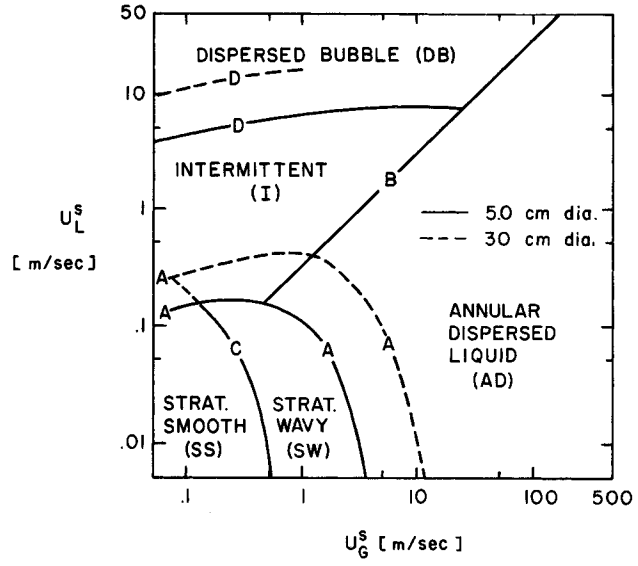

Fig. 7. Effect of fluid properties on transition boundaries. Crude oil-natural gas, 38°C, 68 atm, horizontal.

in diameter could be coordinated on a map in which u_L^s and u_G^s are the parameters. No theoretical basis was given for this method of mapping, and, in fact, the goodness of fit did vary with pipe size and fluid properties. Because the largest part of the data were for 1.3 to 5 cm pipe sizes, the location of the transition boundaries was strongly influenced by these small line size, air-water data. The location of these transition boundaries in the Mandhane map may then be considered a representation of that particular data. Others have also suggested this method of mapping flow regimes (Govier and Omer, 1962).

In order to compare the predictions of the theory given in this paper with the data, the generalized flow boundaries of Figure 4 were recalculated into $u_L^s - u_G^s$ coordinates for the system air-water at 25°C and 1 atm pressure in a 2.5 cm diameter horizontal tube. Once these variables are fixed, F, X, K, and T at each transition boundary are all expressible in terms of the two superficial velocities. The results are shown in Figure 5. The solid curves represent the prediction of the theory presented here. The bands indicate the data (1.3 to 5 cm) represented by the Mandhane boundaries. Very satisfactory agreement exists both with respect to the significant trends of the curves and their absolute locations. Thus it is possible to predict the boundaries as the u_L^s, u_G^s maps from this new theory.

Now that the theoretically based regime transition calculations have been shown to be in good agreement with data, it is possible to explore the effect of design variables with some confidence. Again, by using air-water at 25°C and 1 atm the theoretical predictions of Figure 4 have been recalculated to u_L^s; u_G^s coordinates for 1.25, 5, and 30 cm diameter horizontal pipes. These are shown in Figure 6. Superimposed on each graph are the boundaries recommended by Mandhane which, as indicated above, are based on data for 1.3 to 5 cm pipes. Note that the location of theoretical boundaries B and C are independent of line size. It is seen that for a narrow range of line sizes (say 2 to 5 cm), the location of the boundaries are not very sensitive to the size. However, for the larger sizes such as 30 cm, the displacement of the boundaries is significant. Considerable error will result if a single $u_G^s - u_L^s$ map is used. As expected, for large pipe sizes, the theory predicts that stratified flow will persist to much higher gas rates.

Of considerable practical importance is the flow of oil/natural gas at high pressures where the properties are drastically different than for the air/water case. Flow regime transitions on u_G^s, u_L^s coordinates were calculated for a horizontal pipeline operating at 68 atm and 38°C with oil of density of 0.65 g/cm^3 and natural gas with a density of 0.05 g/cm^3. Viscosities of oil and gas were set at 0.5 and 0.015 cp, respectively. The results for 5 and 30 cm pipe sizes are shown in Figure 7. A comparison with Figures 5 and 6 drawn for air-water shows the inadequacy of assuming that the $u_G^s - u_L^s$ coordinate maps are independent of properties. The transition from smooth to wavy stratified flow and from stratified to annular flow shifts to gas velocities an order of magnitude lower. This is, of course, due to higher gas density. The new theory presented here accounts for these conditions.

The effect of small degrees of inclination on the location of the transitions appears in Figures 8 and 9 as calculated from the generalized theory. The case selected considers air-water at low pressure in a 5 cm diameter pipe. The effect of inclination is very pronounced. Downward inclinations cause the liquid to move more rapidly, have a lower level, and thus require higher gas and liquid flow rate to cause a transition from stratified flows. As shown by comparing Figure 6 with Figure 8, the intermittent flow region shrinks substantially. Conversely, flow with

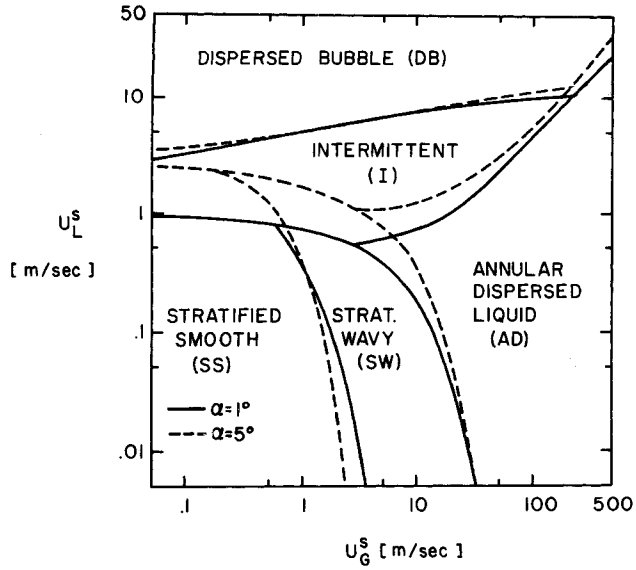

Fig. 8. Effect of inclination on transition boundaries. Water-air, 25°C, 1 atm, 5 cm. diam., downflow.

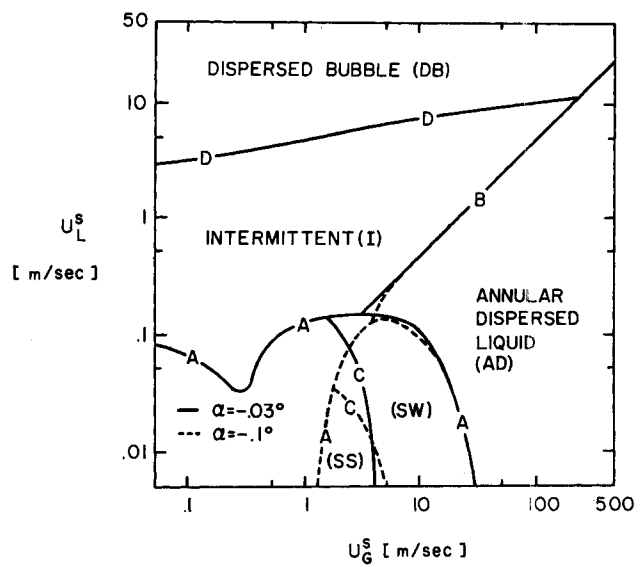

Fig. 9. Effect of inclination on transition boundaries. Water-air, 25°C, 1 atm, 5 cm. diam., upflow.

slight upward angles cause intermittent flow to take place over a much wider range of flow conditions as shown in Figure 9. In fact, at an angle of -0.1 deg., intermittent flow is predicted to take place at extremely low liquid and gas rates. The peculiar shape of the intermittent to stratified transition boundary for $\alpha = -0.03$ deg. is due to a change in the flow from turbulent to laminar.

It should be noted that the generalized map of Figure 4 has been calculated for turbulent flow of both phases. However, as shown in Figure 2, laminar flow of the liquid has little effect on the result.

ACKNOWLEDGMENT

This paper is dedicated to Ovid Baker, who presented the first useful flow regime map. He has been a continuing influence on the research related to two-phase flow problems at the University of Houston.

NOTATION

A = flow cross-sectional area
AD = annular-annular dispersed liquid flow
c = wave velocity
C = coefficient dependent on the size of disturbance, also constant in the friction factor correlation
D = pipe diameter and hydraulic diameter
DB = dispersed bubble flow
f = friction factor
F = modified Froude number, Equation (26)
g = acceleration of gravity
h = liquid level or gas gap
I = intermittent (slug and plug) flow
K = wavy flow, dimensionless parameter, Equation (31)
m = exponent, Equation (5)
n = exponent, Equation (5)
P = pressure
Re = Reynolds number
s = Jeffreys' sheltering coefficient
S = perimeter over which the stress acts, also stratified flow
SS = stratified smooth flow
SW = stratified wavy flow
T = dispersed bubble flow dimensionless parameter, Equation (37)
u = velocity in the x direction
v = velocity normal to the x direction
x = coordinate in the downstream direction
X = Martinelli parameter, Equation (8)
Y = dimensionless inclination parameter, Equation (9)
α = angle between the pipe axis and the horizontal, positive for downward flow
ρ = density
τ = shear stress
ν = kinematic viscosity

Subscripts and Superscripts

G = gas
i = liquid gas interface
L = liquid
s = superficial, for single fluid flow
W = pipe surface
$\sim$ = dimensionless variable
$'$ = disturbed variable
$*$ = friction velocity
$\overline{\ }$ = average

LITERATURE CITED

Agrawal, S. S., G. A. Gregory, and G. W. Govier, "An Analysis of Horizontal Stratified Two-Phase Flow in Pipes," *Can. J. Chem. Eng.*, **51**, 280-286 (1973).

Al-Sheikh, J. N., D. E. Saunders, and R. S. Brodkey, "Prediction of Flow Patterns in Horizontal Two-Phase Pipe Flow," *ibid.*, **48**, 21 (1970).

Baker, O., "Simultaneous Flow of Oil and Gas," *Oil Gas J.*, **53**, 185 (July, 1954).

Benjamin, T. B., "Gravity Currents and Related Phenomena," *J. Fluid Mech.*, **31**, 209-248 (1968).

———., "Shearing Flow Over a Wavy Boundary," *ibid.*, **6**, 161 (1959).

Brock, R. R., "Periodic Permanent Roll Waves," *Proc. Am. Soc. Civil Engrs.*, 96, HYD 12, 2565-2580 (1970).

Butterworth, D., "A Visual Study of Mechanism, in Horizontal, Air Water Flow," *AERE Report M2556*, Harwell, England (1972).

Chu, K. T., "Statistical Characteristics and Modelling of Wavy Liquid Films in Vertical Two Phase Flow," PhD thesis, Univ. Houston, Tex. (1973).

Dukler, A. E., and M. G. Hubbard, "A Model for Gas-Liquid Slug Flow in Horizontal and Near Horizontal Tubes," *Ind. Eng. Chem. Fundamentals* (1975).

Fulford, G. D., "The Flow of Liquids in Thin Films," *Advan. Chem. Eng.*, **5**, 151-236 (1964).

Gazley, C., "Interfacial Shear and Stability in Two-Phase Flow," PhD theses, Univ. Del., Newark (1949).

Govier, G. W., and M. M. Omer, "The Horizontal Pipeline Flow of Air-Water Mixtures," *Can. J. Chem. Eng.*, **40**, 93 (1962).

Hubbard, M. G., and A. E. Dukler, "The Characterization of Flow Regimes for Horizontal Two-Phase Flow," *Proceeding of the 1966 Heat Transfer and Fluid Mechanics Institute*, M. A. Saad and J. A. Moller, ed., pp. 100-121, Stanford University Press, Calif. (1966).
Jeffreys, H., "On the Formation of Water Waves by Wind," *Proc. Royal Soc.*, **A 107**, 189 (1925).
———., "On the Formation of Water Waves by Wind (second paper), *ibid.*, *Proc. Royal Soc.*, **A110**, 241 (1926).
Kordyban, E. S., and T. Ranov., "Mechanism of Slug Formation in Horizontal Two-Phase Flow," *Trans. ASME, J. Basic Engineering*, 92, Series D, No. 4, 857-864 (1970).
Kosterin, S. I., *Izvestiya Akademii Nauk., SSSR., O. T. N.*, **12**, 1824, USSR (1949).
Levich, V. G., *Physicochemical Hydrodynamics*, Prentice-Hall, Englewood Cliffs, N. J. (1962).
Lockhart, R. W., and R. C. Martinelli, "Proposed Correlation of Data for Isothermal Two-Phase, Two-Component Flow in Pipes," *Chem. Eng. Progr.*, **45**, 39-48 (1949).
Mandhane, J. M., G. A. Gregory, and K. Aziz, "A Flow Pattern Map for Gas-Liquid Flow in Horizontal Pipes," *Intern. J. Multiphase Flow*, **1**, 537-553 (1974).
Milne-Thomson, L. M., *Theoretical Hydrodynamics*, The MacMillan Co., New York (1960).
Stewart, R. W., "Mechanics of the Air Sea Interface, Boundary Layers and Turbulence," *Phys. Fluids*, **10**, S47 (1967).
Wallis, G. B., and J. E. Dobson, "The Onset of Slugging in Horizontal Stratified Air-Water Flow," *Intern. J. Multiphase Flow*, **1**, 173-193 (1973).
White, P. D., and R. L. Huntington, "Horizontal Co-Current Two-Phase Flow of Fluids in Pipe Lines," *Petrol. Eng.*, **27**, No. 9, D40 (Aug., 1955).

Manuscript received May 30, 1975; revision received and accepted July 25, 1975.

The Selection of Design Variables in Systems of Algebraic Equations

Present algorithms for the selection of design variables produce a single combination of design variables which results in a solution sequence of minimum difficulty. A new theory entitled *solution mapping* results in information about all optimal combinations of design variables. This theory gives detailed information about the structure of all underspecified systems of algebraic equations which do not contain persistent iteration.

NEIL L. BOOK
and
W. FRED RAMIREZ

Department of Chemical Engineering
University of Colorado
Boulder, Colorado 80302

SCOPE

Typical systems of algebraic equations in steady state, macroscopic design problems have a few characteristics which are dominating factors in the difficulty of obtaining solutions. Usually the equations contain few variables (are sparse) and are nonlinear. Solution strategies for sparse systems of equations are, in general, easily obtained. Conversely, the nonlinearity of the equations increases the difficulty of obtaining a solution.

A general characteristic of a system of algebraic design equations is that the number of variables is equal to or greater than the number of equations. When the number of variables is greater than the number of equations, a set of design variables must be assigned numerical values in order that the system be reduced to a determinant system with an equal number of equations and variables. Judicious selection of design variables can lead to a set of equations whose solution sequence encounters a minimum of difficulty.

Solution sequences for systems of algebraic equations can be separated into three classes: one-to-one or acyclic, simultaneous, and iterative solution sequences. A one-to-one, as opposed to simultaneous or iterative solution sequences, solves each equation, whether linear or nonlinear, in a one at a time technique and does not require any assumed solution points. Systems of equations which can be reduced to a determinant system with a one-to-one solution sequence are said to be without persistent iteration. Any system which cannot be reduced such that it has a one-to-one solution sequence is said to contain persistent iteration.

For systems of algebraic equations without persistent iteration, all one-to-one solution sequences are considered as equal minimum difficulty solution strategies. This is a somewhat arbitrary objective function, since it might be less difficult to solve a set of linear simultaneous equations than a series of acyclic equations for nonlinear elements.

Previous algorithms developed for the selection of design variables in systems of equations without persistent iteration are based on the pioneering work of Steward (1962) which introduced the concept of admissable output sets. An admissable output set has two properties: each equation contains exactly one output variable, and each variable appears as the output element of exactly one equation.

The work by Lee et al. (1966) was one of the earliest attempts to base design variable selection on a mathematical basis. This algorithm operates on a bipartite graph representation for a system of equations and operates only on systems of equations without persistent iteration. The Lee et al. (1966) algorithm was adapted to operate on occurrence matrix representations as presented in Rudd and Watson (1968). This algorithm assigns an admissable output set to a system of equations. The result of the algorithm is a single, optimal combination of design variables and a one-to-one solution sequence for the system of equations.

A system of equations can have many combinations of design variables which will result in one-to-one solution

Correspondence concerning this paper should be addressed to W. Fred Ramirez.